Network-Secure and Price-Elastic Aggregator Bidding in Energy and Reserve Markets

Ahmad Attarha, *Student Member, IEEE*, Paul Scott, José Iria, and Sylvie Thiébaux, *Member, IEEE*

***Abstract*—The increasing uptake of distributed energy resources (DER) is displacing the dispatchable generators responsible for providing frequency response in our power system. To compensate for the withdrawal of such generators, the market participation of DER fleets through aggregators has been suggested in the literature. Unfortunately, these works are either limited to price-taking aggregators or neglect the distribution network. The first limitation leads to inelastic bids which do not reflect DER flexibility, while the second results in bids that do not lie within the network boundaries. To mitigate these challenges, we propose a price-elastic aggregator bidding approach together with a network conforming layer. Our approach enables aggregators to offer a range of network-secure bid bands for different prices. To preserve the independent role of each stakeholder and share the computational burden, we decompose the problem into aggregator and network subproblems, solved sequentially. Moreover, we confer aggregators the possibility to provide reactive power support to enable the network to accept greater throughput. Finally, since our approach ensures network feasibility prior to bids reaching the market, it minimizes the disruption to existing wholesale market structures. Our results on a 141-bus network shows 19% higher benefits for aggregators, compared to the inelastic bidding approach.**

***Index Terms*—Aggregators, distribution network, electricity market, FCAS, OPF.**

NOMENCLATURE

Indices and Sets

$\mathcal{K} \in T$	Set of rolling horizons
$a \in A$	Set of aggregators
$b \in B$	Set of bid bands
$i, j, k \in N$	Set of network nodes
$m \in M$	Set of segments within the piecewise linear function ω.
$n \in C_i^a$	Set of consumers being served by aggregator a at node i
$t, \tau \in T$	Set of time steps.

Parameter

$\bar{\pi}_t^e, \bar{\pi}_t^r, \bar{\pi}_t^l$	Energy, FCAS raise and lower price forecasts (\$/kWh/\$/kW)
$\bar{P}_{i,t}^{\mathcal{K}-1}$	Network limits at rolling horizon $\mathcal{K}-1$ for node i and time t (kW)
δ	Duration of time steps in hours (h)
γ	Battery replacement cost (\$)
$\underline{v}^2, \bar{v}^2$	Squared voltage safe upper and lower bounds (p.u.)
μ_t^l, μ_t^r	Probability of a raise/lower contingency
σ	Battery efficiency
PV_t^F, P_t^l	PV power and inflexible load forecasts (kw)
q_i^a	Background reactive power of aggregator a at node i (kVar)
$R, \underline{E}, \overline{E}$	Battery charge/discharge rate, upper and lower SoC bounds (kw)
r_i, x_i, z_i	Resistance, reactance and impedance of line between node i and its upstream (p.u.)
S^{pv}, S^{batt}	Apparent power limits for solar and battery inverters (kVA)
S_{base}	Apparent power base value (100 kVA).

Variables

α	Discharging depth of the battery.
$\lambda_i \in \mathbb{R}$	Curtailment at node i (p.u.)
$\pi_b^e, \pi_b^r, \pi_b^l$	Energy, raise and lower price for capacity band b (\$/kWh/ \$/kW)
F_i^e, Q_i^e, I_i^e	The active, reactive power and the squared current magnitude flowing into node i from its upstream for the energy market (p.u.)
$P_i'^e$	Overall energy bid accepted by the DSO at node i (p.u.)
p_t^e, p_t^r, p_t^l	Energy, raise and lower FCAS bids of a consumer (kW)
$P_{i,t}^{a,e}, P_{i,t}^{a,r}, P_{i,t}^{a,l}$	Total energy, raise and lower FCAS bids of aggregator a at node i (kW)
P_t^{ch}, P_t^{dis}, E_t	Battery charge, discharge, SoC (kW/kWh)
P_t^{pv}, Q_t^{pv}	Active, reactive power output of a PV system (kW/kVar)
$Q_i'^e$	Reactive power used by network to expand its feasible region (p.u.)
$Q_{i,t}^a$	The reactive power support of aggregator a at node i and time t (kVar)
Q_t^{batt}	Reactive power output of a battery inverter (kVar)

Manuscript received July 15, 2020; revised November 9, 2020; accepted December 29, 2020. Date of publication January 6, 2021; date of current version April 21, 2021. This work was supported by the Australian Renewable Energy Agency (ARENA), as part of ARENA's Advancing Renewables Program through the Project "Optimal DER Scheduling for Frequency Stability." Paper no. TSG-01092-2020. *(Corresponding author: Ahmad Attarha.)*

The authors are with the College of Engineering and Computer Science, Australian National University, Canberra, ACT 2026, Australia (e-mail: ahmad.attarha@anu.edu.au; paul.scott@anu.edu.au; jose.iria@anu.edu.au; sylvie.thiebaux@anu.edu.au).

Color versions of one or more figures in this article are available at https://doi.org/10.1109/TSG.2021.3049464.

Digital Object Identifier 10.1109/TSG.2021.3049464

u_t	Binary auxiliary variable
V_i	Squared voltage magnitude at node i (p.u.)

I. Introduction

A. Research Motivation

THE ADVENT of distributed energy resources (DER), such as rooftop PV and batteries, is cutting down the market share of big generating companies, with a notable fraction of the overall demand being supplied by consumers. This adoption of DER and grid-scale renewable projects translates to fewer dispatchable generators for market operators to ensure the safe operation of their power systems.

Recently, the market participation of residential DER through aggregators has been suggested as a promising approach to provide market operators with more flexibility. Despite this intention, the state of the art has mainly simplified aggregators' bidding to just a single band. In other words, existing approaches optimize aggregators' resources according to a price forecast and bid the obtained schedule at either market floor or cap prices. Assuming that the market does not reach its floor or cap prices, these bids are fully cleared, hence, we call them *inelastic* bids. Such a simplification not only narrows the DER flexibility down to a single band, but also can reduce aggregators' benefit when the market clearing price (MCP) deviates from the forecast. On the contrary, bidding a wider range of DER flexibility at different price bands enables aggregators to fully exploit their capabilities and hedge the price uncertainty effect which will benefit both aggregators themselves and the market as a whole.

However, bidding the available operating range of DER, rather than just a single band, generates some new challenges not encountered by the inelastic approaches. One of these new challenges is the inter-dependency between the energy and the reserve markets, where the participation in one market can limit the bids in another. In fact, when bidding the full operating range of DER, aggregators need to obtain a feasible region accounting for any energy and reserve dispatch combinations. Another challenge is to ensure that the distribution network will not be overloaded by aggregator actions. Since aggregators bid a feasible region, the network also requires calculating its feasible operating region. The privacy concerns as well as the independent role of the aggregators and the distribution system operator (DSO) will also add to the complexity of such a problem.

To solve the above challenges, we introduce a new price-elastic bidding approach in which aggregators and the DSO solve their respective subproblems sequentially. The aggregator subproblem of our approach has aggregators calculate their energy-reserve feasible operating regions, the marginal prices for a series of capacity bands within these operating regions, and finally the reactive power support capacity (which can be injected/absorbed by inverters). In the network subproblem, the DSO calculates the network operating region and shapes the aggregator bids to be within these limits. As part of this the DSO can use reactive power to increase network throughput. The aggregators can then submit their network-constrained bids to the wholesale market.

B. Related Work

The uptake of smart technologies at the demand side (i.e., smart controllers and smart meters) with the ability to communicate to an aggregator have enabled consumers to respond to real-time prices and participate in electricity markets [1]. This is why the participation of residential DER in either energy [2], [3], and/or reserve markets [4]–[8] has attracted notable attention in the literature. In [2]–[8], a third party (e.g., an aggregator) optimizes/co-optimizes DER according to a price forecast to obtain inelastic bids for the wholesale markets. References [2]–[8] assume that the market actions of aggregators do not violate the operational limits of the grid. However, the often synchronous behavior of DER, e.g., in response to a price spike or during peak PV production, can exceed the network boundaries and thus can lead to infeasibilities.

To avoid network infeasibility, [9]–[12] enhance their models by taking the distribution network constraints into account. Similarly to [2]–[8], the works [9]–[12] also rely on generating inelastic bids. Such an inelastic bidding policy simplifies the network inclusion as the operating state of the network can be known and checked prior to submitting bids to the wholesale market.[1] Therefore, they either solve centralized [9]–[11], or decentralized OPFs [12] to ensure the network feasibility for this pre-known operating point.

However, with or without network consideration, the inelastic bidding approaches, [2]–[12], can negatively affect both the market and aggregators. From the market perspective, inelastic bids always need to be settled (as long as the market does not reach its cap or floor prices). Therefore, the market is constrained to dispatch these DER bids at a predetermined operating point, despite the underlying flexibility of DER.

For aggregators on the other hand, restricting DER to operate at one point (as in inelastic approaches [2]–[12]) not only misses opportunities for providing higher value market services but also can lead to economic loss in cases where cleared electricity prices deviate from forecasts.

To avoid these problems, we instead propose generating price-elastic bid bands that account for an aggregator's full feasible operating region. Since the participation in one market might change their capability in another, we calculate an aggregator's energy-reserve region accounting for these inter-dependencies. We also obtain the marginal prices of getting dispatched at different bands across this energy-reserve region. When bidding a range of DER operating bands at different prices, the final operating point of the aggregators and thus of the distribution network will depend on the market output. Therefore, unlike the inelastic bidding approaches [9]–[11]), here, there is no single pre-known operating point to run an OPF and ensure the network feasibility. To meet this challenge, we propose obtaining the network operating region using a series of multi-period OPFs. We then restrict aggregators' feasible regions to be within the network operating region, in a way that favors more competitive aggregator bids. This reduces the operation cost of the whole system which is in line with

[1]Remember that inelastic participants are assumed to get fully dispatched as they bid at either market cap or floor prices.

TABLE I
PROPOSED APPROACH VS. RELATED WORK

Ref.	Raise & Lower Reserve	Network Full Info.	Reactive Power	Bidding Type
[2], [3]	No	No	No	Inelastic
[4]–[8]	Yes	No	No	Inelastic
[9]–[12]	Yes	Yes	No	Inelastic
[13]	No	No	No	Price Elastic
[14]–[16]	Yes	No	No	Inelastic
Proposed	Yes	Yes	Yes	Price Elastic

the objective of both the market and the DSO. Additionally, our network model ensures network security for any market clearance output.

The intrinsically distributed nature of the problem, sensitivity of private participant data, computational effort, and uncertain forecasts, all contribute to increasing the difficulty of the problem. We address these by decomposing the problem and solving it over a rolling horizon. Our approach divides the problem into aggregator and network subproblems, that are sequentially solved by each entity. Unlike [9]–[11], our setting allows sharing the computational burden amongst all the parties which can significantly decrease the runtime through the use of parallel computing. These subproblems are solved within a rolling horizon that moves forward in lock with the real-time market. This ensures that aggregators put their best offers forward, which incorporate the latest and most accurate forecasts over their uncertain parameters, and incorporate the realization of their stateful variables.

This article builds on our conference paper [13], by extending it in three main ways. Firstly, we enable aggregators to participate in both raise and lower reserve markets leading to a higher aggregator profit. Secondly, our approach provides aggregators with the possible future network congestion information, which helps aggregators make informed decisions. Finally, unlike [2]–[13], we enable aggregators to provide reactive power capacity to the network. The network can use this reactive power to expand its feasible region leading to aggregators participating in the market with less network limitations.

To the best of our knowledge we are the first to propose such a price-elastic bidding approach for residential DER. Even for the grid-scale DER, most research, such as [14], has relied on inelastic bidding policies. The few exceptions that consider the market price variation, such as [15] and [16], take the sensitivity of the price into account, but still ultimately submit an inelastic bid. In other words, rather than using a price forecast, they obtain a modified price upon which they generate inelastic bids. Thus, in addition to excluding network constraints, [14]–[16] are not able to offer a range of DER flexibility for different prices. Table I summarizes the main differences of our proposed approach with the related literature. This comparison is in terms of whether both raise and lower reserve market are considered (shown by Raise & Lower Reserve in Table I), whether aggregators are provided with the forecasts of future network congestion (shown by Network Full Info) and whether aggregators provide the network with their reactive power support (shown by Reactive Power).

Given the above literature, our contributions are:

- A novel price-elastic aggregator bidding approach for energy and reserve markets, which more accurately captures the flexibility and value of DER, and enables DER dispatch to adjust to the uncertain realization of market prices.
- A new network optimization layer that jointly conforms price-elastic energy and reserve bids within distribution network limits, while encouraging competition between aggregators. This is done prior to bids reaching the market, to avoid disruption to existing market structures, enabling the approach to be more readily taken up.
- Enabling aggregators to provide reactive power voltage support, alongside energy and reserve bidding, in order to achieve greater network throughput and greater aggregator access to wholesale markets.

Note that we develop our approach under the Australian national electricity market (NEM) regulations, operated by the Australian energy market operator (AEMO). In line with the NEM and AEMO terminology, here-after, we use the term "frequency control ancillary service" (FCAS) instead of reserves and "FCAS market" for the market in which FCAS is traded. Despite this focus, our approach is widely applicable for participation in markets that co-optimize energy and reserves bids, such as CAISO, ERCOT, PJM [17].

The rest of this article is organized as follows: after briefly introducing the NEM and AEMO in Section II, we provide an overview of our network-secure price-elastic approach in Section III. We then introduce the aggregator and network subproblems of our approach respectively in Sections IV and V. We numerically illustrate the effectiveness of our approach in Section VI. Finally, we conclude this article in Section VII.

II. NATIONAL ELECTRICITY MARKET

The NEM is a wholesale spot market within which the energy and FCAS markets are fully co-optimized every five minutes using the NEM dispatch engine (NEMDE). The FCAS market includes both regulation and contingency services. The contingency FCAS market is further broken down into markets for 6-second, 60-second, and 5-minute response times. To ensure safe operation, AEMO secures every 5-minute interval with enough raise and lower support from each FCAS market (regulation and every contingency FCAS market) [18].

The NEM requires participants to submit their energy-FCAS region, known as a *trapezium* for its geometry, which can be submitted with up to 10 price-bands for each market. An example energy and FCAS trapezium submitted for a generator is shown in Fig. 1. This notifies the market that the generating unit can be dispatched at any point within the trapezium (highlighted in yellow in Fig. 1), for the right price.

Although all participants get dispatched in the real-time market, they are required to submit their bids (feasible regions and 10 price-bands) one day in advance. This enables AEMO to predict and resolve the real-time shortages. Currently, while the price-bands cannot be updated in real-time, the capacity can be modified at each 5-minute interval. Here, we only deal with the real-time part of the problem, yet one can use

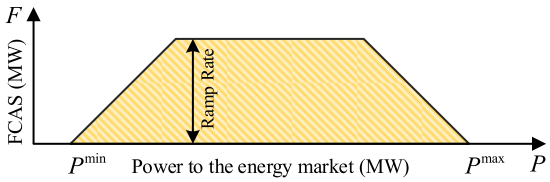

Fig. 1. Energy-FCAS trapezium for a generating unit.

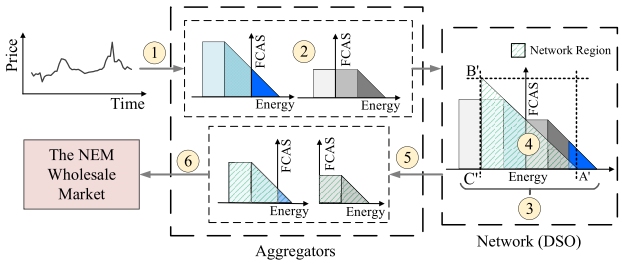

Fig. 2. Schematic overview of our price-elastic approach.

our approach a day before to generate the prior-day bids. Moreover, we investigate a more general case in which the price bands can also be updated in real-time. We explore the effect of fixed prices in the result section.

III. The Overall Approach

Figure 2 illustrates how our network-secure price-elastic approach interacts with the NEM wholesale market. Every 5 minutes, participating aggregators receive (or calculate) a new wholesale market price forecast over a forward horizon (shown by ① in Fig. 2). The aggregators use this price forecast as a basis for calculating multi-band bids (represented in the NEM as bid trapeziums) for the next 5 minute dispatch interval, and for each node of the distribution network where they have customers ②. The network takes these bids, merges them to obtain a polygon at each node ③, and solves a set of OPFs and curtails the bids to obtain an overall bid region that will always remain within the network limits for any combination of ways in which the wholesale market could dispatch energy and reserve ④. The curtailments are then applied to the original aggregator bids in the order of the least to the most competitive (in terms of price) bids ⑤, before being sent to the wholesale market for consideration ⑥.

In this overall approach, aggregators are free to calculate their multi-band bids as they please, as long as it conforms to the bidding structure. In this article, we propose a particular method, based on the fact that in a competitive and efficiently operating market, the bids of participants will tend toward reflecting their true underlying costs and constraints. The bidding requirements of existing markets are not expressive enough to capture these underlying requirements of participants to high accuracy, so we will have to allow for some assumptions and approximations in this process.

For the network subproblem, when the DSO has to make a decision between two bids (i.e., if the combination of them would lead to a network violation), all else being equal, it will opt for the bid with the more competitive price offering. The idea is that the wholesale market would favor this bid over the less-competitive one in order to achieve an efficient dispatch, so we should similarly be offering the most competitive subset of bids that will remain within the network's limits.

We implement our approach within a rolling horizon framework which moves forward every 5 minutes. This allows aggregators to account for the gradual revelation of uncertainty and include the latest (most accurate) uncertainty information into their optimization problem. While we expect a fairly accurate PV forecast for the next 5-minute interval, we are not prescribing that aggregators solve a deterministic optimization problem to obtain their bids. In fact, our overall approach does not stop aggregators from taking a stochastic/robust approach into consideration when generating their feasible regions (trapeziums). In the following, we present the aggregator and network subproblems for iteration $\mathcal{K}$ of our rolling horizon framework.

IV. Aggregator Sub-Problem

Here, we first model HEMS (home energy management system) of a consumer owning a battery, PV and a background load[2] in Section IV-A. Next, we develop a model to enable aggregators to schedule their consumers in Section IV-B. We then use such an HEMS model as well as the aggregators' co-optimization problem as bases to build our price-elastic aggregator subproblem.

A. Consumer HEMS Problem

Here, we divide the consumer constraints into two groups: constraints that tie the bids for different markets, and those modeling the operational bounds of the consumers' DER.

1) Market Coupling Constraints: We combine the energy p_t^e, raise $p_t^r \geq 0$ and lower $p_t^l \geq 0$ FCAS bid variables of the consumers in a vector p_t for later reference. We use p_t^+ and p_t^- to respectively link the raise and lower markets with the energy as follows:

$$p_t^+ = p_t^e + p_t^r, \qquad p_t^- = p_t^e - p_t^l. \tag{1a}$$

2) DER Variables and Constraints: DER constraints should be satisfied for energy (i.e., p_t^e) and FCAS delivery scenarios (i.e., p_t^+ and p_t^-). Here, we only present the DER variables and constraints for the energy scenario; the same variables and constraints are then duplicated for raise and lower FCAS market scenarios.

Rooftop PV: Rooftop PV has a variable for active power $P_t^{pv} \in [0, PV_t^F]$; as well as a variable for the reactive power Q_t^{pv} (provided by its inverter) which is obtained as follows:

$$Q_t^{pv2} = S^{pv2} - P_t^{pv2}. \tag{1b}$$

Battery: Battery charge and discharge variables are linked to the state of charge (SoC) variable $E_t \in [\underline{E}, \overline{E}]$ as follows:

$$E_t = E_{t-1} + \delta\left(\sigma P_t^{ch} - P_t^{dis}/\sigma\right) \tag{1c}$$

[2]It is it is relatively straightforward, depending on the convexity of the model, to include any load type into the consumer subproblem, such as thermostatically controllable loads. However, to clearly explain the underling idea behind our approach, here, we only model PV and batteries.

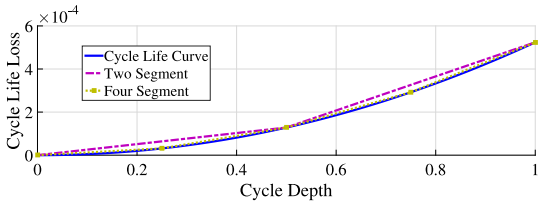

Fig. 3. Approximation to the cycle depth aging stress function.

where:

$$0 \leq P_t^{ch} \leq R \cdot u_t \tag{1d}$$

$$0 \leq P_t^{dis} \leq R \cdot (1 - u_t) \tag{1e}$$

The auxiliary binary variable u_t is added to avoid simultaneous battery charging/discharging. Note that the bids made to the FCAS markets are capacities which might not get deployed. Therefore, we use the latest SoC (i.e., E_{t-1}) from the energy scenario to model the SoC constraint for both raise and lower FCAS at each time t.

To take the battery degradation cost into account, we use the MILP model introduced in [19]. In line with [19], we obtain the cost associated with the cycle of depth α using the depth stress function $\Psi(\alpha)$. The depth of battery cycle at time t can be obtained as follows:

$$\alpha_t = \frac{1}{\sigma \cdot \overline{E}} \cdot P_t^{dis} + \alpha_{t-1} \tag{1f}$$

The marginal cycle aging is obtained by taking the derivative of $\Psi(\alpha_t)$ w.r.t P_t^{dis}. This can be written as follows:

$$\frac{\partial \Psi(\alpha_\tau)}{\partial P_t^{dis}} = \frac{d\Psi(\alpha_\tau)}{d\alpha_\tau} \frac{\partial \alpha_\tau}{\partial P_t^{dis}} = \frac{1}{\sigma \cdot \overline{E}} \frac{d\Psi(\alpha_\tau)}{d\alpha_\tau} \tag{1g}$$

To define the marginal cost of cycle aging, we prorate the battery replacement cost $\gamma(\$)$ to the marginal cycle aging, and build a piece-wise linear function ω. This function has M even segments dividing the cycle depth range from 0 to 100%.

$$\omega(\alpha_t) = \begin{cases} \omega_1, & \text{if } \alpha_t \in [0, \frac{1}{M}) \\ \vdots & \\ \omega_m, & \text{if } \alpha_t \in [\frac{m-1}{M}), \frac{m}{M}) \\ \vdots & \\ \omega_M, & \text{if } \alpha_t \in [\frac{M-1}{M}), 1]) \end{cases} \tag{1h}$$

where

$$\omega_m = \frac{\gamma}{\sigma \cdot \overline{E}} M \left[\Psi\left(\frac{m}{M}\right) - \Psi\left(\frac{m-1}{M}\right) \right] \tag{1i}$$

Fig. 3 shows the cycle depth stress function and its piece-wise linearisation for different numbers of segments.

Finally, we obtain the cycle aging cost Ω_t by summing the cycle aging costs associated with each segment as follows:

$$\Omega_t = \sum_{m \in M} \delta \cdot \omega_m \cdot P_{t,m}^d \tag{1j}$$

where $P_t^{dis} = \sum_{m \in M} P_{t,m}^d$. We use $\Omega_{c,t}$ for the aging cost of consumer c which is used in the aggregator objective function. As a result, aggregators will take their battery aging cost into account when bidding to the electricity market.

The reactive power support Q_t^{batt} the battery can exchange with the grid using its inverter can be obtained as:

$$Q_t^{batt^2} = S^{batt^2} - P_t^{ch^2} - P_t^{dis^2}. \tag{1k}$$

Combined Power: A consumer's power exchange with the energy market is:

$$p_t^e = P_t^{dis} - P_t^{ch} + P_t^{pv} - P_t^I \tag{1l}$$

Note that the forecasts (i.e., PV_t^F and P_t^I) can be updated with the latest and the most accurate values as our rolling horizon framework moves forward.

Overall, the HEMS problem includes the market coupling constraint (1a), and 3 copies of consumer's variables and constraints (1b)–(1l), one for each output case: p_t^e, p_t^+ and p_t^-. Note that (1b)–(1l) provide all the required bounds on our variables including up and down reserve limits. Note that there is no objective function in the HEMS model as the consumers are scheduled according to the aggregator's objective. In this article, the objective of aggregators is to maximize the benefit of co-participating in energy and reserve markets. Therefore, aggregators receive consumers' constraints (presented above) and co-optimize them for energy and reserve market as explained in the following section.

B. Aggregator Energy-Reserve Co-Optimization Problem

We combine the variables for total energy $P_{i,t}^{a,e}$, raise and lower FCAS bids $P_{i,t}^{a,r}$, and $P_{i,t}^{a,l}$, in a vector $P_{i,t}^a$ for the sake of presentation. We index $p_t = (p_t^e, p_t^r, p_t^l)$ with c to represent the bid vector of consumer c. Given the energy, FCAS raise and lower price forecasts, $\bar{\pi}_t = (\bar{\pi}_t^e, \bar{\pi}_t^r, \bar{\pi}_t^l)$, aggregator a solves the following problem:

$$\max_P \sum_{i \in N} \sum_{t \in T} \delta \cdot \bar{\pi}_t \cdot P_{i,t}^a - \sum_{c \in C_i^a} \sum_{t \in T} \Omega_{c,t} + \sum_{c \in C_i^a} \sum_{t \in T} D_{c,t} \tag{2a}$$

$$P_{i,t}^a = \sum_{c \in C_i^a} p_{c,t} \quad \forall i \in N, t \in T \tag{2b}$$

$$\text{(1a) and 3 copies of (1b)–(1l)}, \qquad \forall c \in C^a \tag{2c}$$

The first term in the objective function maximizes the benefit of aggregators in energy and FCAS markets. The second term adds the battery degradation cost obtained via (1j) and the third term adds the reserve deployment cost $D_{c,t}$ obtained as:

$$D_{c,t} = \bar{\pi}_t^e \cdot \delta' \left(\mu_t^r \cdot p_{t,c}^r - \mu_t^l \cdot p_{t,c}^l \right) \tag{2d}$$

where δ' is the worst case number of seconds we would need to be deployed for a single contingency. Equation (2d) models the probability of a contingency event occurring for lower and raise reserves μ_t^l and μ_t^r, while assuming that the value of the lost/gained energy is at the energy market price $\bar{\pi}_t^e$. The significance of these deployment costs shrinks to zero as contingencies become more rare. Note that this optimization problem is what an inelastic approach uses to obtain the bids according to the forecasts.

In the following, we use the above co-optimization problem to obtain the three important parts of our aggregator subproblem, i.e., the energy-reserve regions (Section IV-C), up to 10 price-bands (in the NEM) across their feasible

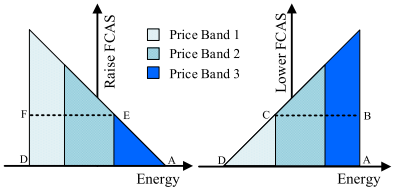

Fig. 4. Feasible region of an aggregator with 3 price-bands.

region (Section IV-D) and finally the reactive power they can exchange with the grid for network support purposes (Section IV-E).

C. Aggregator Feasible Region

Since the aggregators mainly own inverter-based DER technologies, their overall energy-FCAS region has the shape of a triangle as shown in Fig. 4. This is because, unlike a general trapezium (e.g., Fig. 1), their feasible region will not be limited by ramp rates [20]. However, irrespective of ramp rates, aggregators[3] might want to bid a trapezium as some of their consumers might either not participate or only partially participate in the FCAS market. Such a partial market participation brings consumers' preferences into our model. Therefore, in this article, we do not limit an aggregator's feasible region to a triangle. In fact, aggregators can bid a trapezium shown by (A, B, C, D) for lower and (A, E, F, D) for raise FCAS market. In the following we use (2a)–(2c) to obtain the coordinates of points A–F and thus aggregator feasible regions.

1) Point A: To get the coordinates of point A, we maximize the energy market participation of the first time step as follows:

$$P_{i,1}^{a,e(max)} := \max \sum_{i\in N} P_{i,1}^{a,e} \tag{3a}$$

$$\text{s.t.} \quad (2b)-(2c) \tag{3b}$$

Thus, $(P_{i,1}^{a,e(max)}, 0)$ is the coordinates associated with point A in Fig. 4.

2) Point B: To get point B, we maximize the lower FCAS market participation of the first time step as follows:

$$P_{i,1}^{a,l(max)} := \max \sum_{i\in N} P_{i,1}^{a,l} \tag{4a}$$

$$P_{i,1}^{a,e} = P_{i,1}^{a,e(max)} \quad \text{s.t.} \quad (2b)-(2c) \tag{4b}$$

Thus, B= $(P_{i,1}^{a,e(max)}, P_{i,1}^{a,l(max)})$. We obtain the other points in a similar fashion but omit this here for the sake of brevity.

D. Price Bands

Aggregators' stateful technologies, such as batteries, make a profit by arbitraging energy. Thus, obtaining representative price-bands for aggregators relies on the price and dispatch over time, yet, this information is not available to aggregators as the NEM clears only one step at a time. Therefore, to make sound decisions, we need to reflect the expected future benefit when making decision in the first time step. To do so, we select b capacity bands (up to 10 in the NEM) across the energy-reserve region in the first time step ($t = 1$) at horizon $\mathcal{K}$. In fact, these bid bands are possible dispatch scenarios, each of which can lead to a different future schedule. We then obtain the schedule and the future benefit associated with getting dispatched at each band. Comparing the future benefit of each band with a base case (in which aggregators only have their consumers background load), we obtain the minimum price for delivering that capacity.

Note that since the aggregator and network subproblems are solved sequentially, the latest network limits will be imposed to our bids later on when solving the network subproblem (Section V). However, to ensure that the aggregator subproblem does not completely neglect the future network congestion, we enforce the network limits $\bar{P}_{i,t}^{\mathcal{K}-1}$ obtained at the previous iteration (i.e., $\mathcal{K}-1$) into the planning time steps (i.e., $2 \le t \le T$) of the aggregator subproblem solved at iteration $\mathcal{K}$. We do not impose the network limits for $t = 1$ since such limits will be imposed in the upcoming network subproblem. This ensures that the first time step (which will be submitted to the market) is not inaccurately bounded based on the previous horizon. Let $P_{i,t=1}^{b}$ denote the dispatch at price-band b, i.e., energy, maximum raise and maximum lower at the b-th segment of the energy-reserve region. The expected future benefit $\mathcal{B}_{exp}^{b}$ associated with $P_{i,t=1}^{b}$ is obtained as follows:

$$\mathcal{B}_{exp}^{b} := \max \sum_{t\in\{2,\dots,T\}} \Big(\sum_{i\in N} \delta \cdot \pi_t \cdot P_{i,t}^{a} + \sum_{c\in C_i^a} (D_{c,t} - \Omega_{c,t})\Big) \tag{5a}$$

$$P_{i,t=1}^{a} = P_{i,t=1}^{b} \tag{5b}$$

$$P_{i,t}^{a} \le \bar{P}_{i,t}^{\mathcal{K}-1} \forall i \in N, t \in \{2,\dots,T\} \tag{5c}$$

$$(2b)–(2c) \tag{5d}$$

Having obtained the expected future benefit associated with every band b, we need to transfer them into reasonable prices. To do so, we compare the total benefits (first time step + future benefit) of getting dispatched at each capacity band with a base case ($b = 1$) where consumers are just withdrawing their background load from the grid in the first time step. The price of getting dispatched at each capacity band should be such that aggregators obtain higher benefits than in the base case (since otherwise they should get dispatched at the base case). Let $\pi_b = (\pi_b^e, \pi_b^r, \pi_b^l)$ denote the energy, raise and lower price for capacity band b. Given $P_{i,t=1}^{b}$, $P_{i,t=1}^{b=1}$ and their future benefits $\mathcal{B}_{exp}^{b}$, $\mathcal{B}_{exp}^{b=1}$, this can be written as:

$$\delta \cdot \pi_b (P_{i,t=1}^{b} - P_{i,t=1}^{b=1}) + \mathcal{B}_{exp}^{b} \ge \mathcal{B}_{exp}^{b=1}. \tag{6}$$

Note that (6), in the marginal case, can be simplified to: $a\pi_b^e + b\pi_b^r + c\pi_b^l = d$ where a, b, c, and d are constants. Such an equation can be satisfied for an infinite combination of energy and FCAS prices. To limit this and obtain a unique solution, w.l.o.g., we fix the FCAS prices to zero and obtain the energy price for which the aggregator can operate at band b in the energy market and provide the associated FCAS capacities. Note that even though the bids for each market are

[3]Note that our overall approach enables even a single consumer (i.e., 1 aggregator = 1 consumer) to directly bid to the wholesale market (i.e., our approach is still able to shape their bids to ensure the network security).

separate, in practice, the market cost function will be inseparable in NEMDE. Therefore, while it produces a unique solution for (6), it will not change the aggregators' dispatch.

E. Aggregator Reactive Power Support

Here we obtain the reactive power the aggregator can exchange with the grid to provide a greater network throughput. We index Q_t^{pv} and Q_t^{batt} with c to show the reactive power support provided by the inverter of PV and battery of consumer $c \in C_i^a$. Therefore, the reactive power of the aggregator for the network support $Q_{i,t}^a$ is obtained as follows:

$$Q_{i,t}^a \leq \sum_{c \in C_i^a} \left[Q_{c,t}^{pv} + Q_{c,t}^{batt} \right] \quad \forall i \in N, t \in T \tag{7}$$

As explained in Section IV-A, Q_t^{pv} and Q_t^{batt} are just for the energy scenario. Therefore, the same variables and constraint should be duplicated for the raise and lower FCAS scenarios. Moreover, here, we assume that the aggregators are not paid for their reactive power support and their only benefit in providing such a support is to diminish network restrictions. This is also inline with the Australia/New Zealand standard where the inverters are required to be able to provide reactive power support for the distribution network. However, such services can be contracted and paid for. This does not change our approach and will just increase aggregators' benefit.

Having obtained the feasible regions, prices and the reactive power support, aggregators communicate them with the DSO to have their bids shaped. Note that aggregators participating in other co-optimized markets that do not require a trapezium, can use a similar process to generate multiple bands and submit them to the DSO/market in the spirit of multiple simple bids.

V. Network Sub-Problem

The goal of our network subproblem is to open up as much network capacity as possible for aggregators while ensuring grid security. To achieve this, we first merge aggregators' feasible regions to have a polygon at each network node, i.e., $\mathcal{P}_i^e = \sum_{a \in A_i} P_i^{a,e} / S_{base}$. For every extreme point[4] of the overall polygon (i.e., $\mathcal{P}_i^{e,Ex}$), our network subproblem takes the total desired capacity, solves an OPF and then returns a curtailment λ_i for each node. To reduce the total operation cost, we apply this curtailment to the bids from least to the most competitive (in terms of price) and curtail in this order until we have curtailed the total of λ_i at each node.

In the following, we use the branch flow equations [21] to model the distribution network constraints for the energy market; we duplicate similar constraints for the raise and lower FCAS scenarios [12]. Since there is no time coupling constraint in the network subproblem (unlike in the aggregator subproblem due to battery SoC), the OPF problem of each time-step t can be solved separately and in parallel. Thus, here, we drop the index t to increase readability. The network subproblem is modeled as:

$$\min \sum_{i \in N} ||\lambda_i||_2^2 \tag{8a}$$

$$F_i^e - r_i I_i^e + P_i'^e = \sum_{j \in D_i} F_j^e \qquad \forall i \in N \tag{8b}$$

$$Q_i^e - x_i I_i^e + \sum_{a \in A_i} q_i^a + Q_i'^e = \sum_{j \in D_i} Q_j^e \qquad \forall i \in N \tag{8c}$$

$$V_i^e = V_k^e - 2\left(r_i F_i^e + x_i Q_i^e\right) + z_i^2 I_i^e \qquad \forall i \in N \tag{8d}$$

$$\underline{v}^2 \leq V_i^e \leq \bar{v}^2 \qquad \forall i \in N \tag{8e}$$

$$F_i^{e\,2} + Q_i^{e\,2} = V_i^e I_i^e \qquad \forall i \in N \tag{8f}$$

$$0 \leq I_i^e \leq \bar{i}_i^{\,2} \qquad \forall i \in N \tag{8g}$$

$$P_i'^e + \lambda_i = \mathcal{P}_i^{e,Ex} \qquad \forall i \in N \tag{8h}$$

$$Q_i'^e \leq \sum_{a \in A_i} Q_i^a / S_{base} \qquad \forall i \in N \tag{8i}$$

The objective (8a) minimizes the square L2 norm of the bid curtailments. Since we apply the bid curtailment from the least to the most competitive price order, the more curtailment occurs at any one particular node, the more likely we will start to curtail competitive bids. When the curtailment is more evenly spread across many nodes, as with the L2 norm, we will tend to just curtail the least-competitive bids at each node. An L1 norm curtailment policy has been used in the literature to limit PV systems, e.g., [22]. However, such an L1 norm policy, curtails the bids at weaker nodes (mainly end nodes) until the network problem is fixed. Thus, at these nodes, both the least and the most competitive bids will be curtailed. In the results section, we will illustrate the difference between the two norms and show that L2 norm is more appropriate.

Active and reactive power flow equations are given by (8b)–(8c), where, D_i and A_i are the child nodes and the set of aggregators at node i; (8d) obtains the squared voltage magnitude V_i at each node, which is enforced to be within its bounds in (8e). Equation (8f) gives the line's complex power; The current flowing in each line is bounded via (8g). The overall bid accepted by the network plus the bid curtailment is enforced to be equal to the overall aggregator bid in (8h). Finally, the reactive power used by the network is limited to aggregators reactive power offer through (8i).

Note that (8a)–(8i) need to be solved for the extreme points on the energy, raise and lower FCAS axis. As shown in Fig. 2, the feasible regions accepted by the network might be smaller than the one aggregators have provided. Finally the shaped bids are submitted to the market. When the market is cleared, each aggregator finds out where in their bid trapezium they will be dispatched for the upcoming interval. From here on, our approach is repeated with updated inputs.

VI. Numerical Results

A. Setup and Data

To examine the performance of our proposed price-elastic approach, we use a 141-bus distribution network modified with 10 consumers at each node (1410 consumers in total). To better reflect the real-world DER penetration and obtain a more

[4]The obtained polygon includes several bid scenarios. However, we only need to explore the worst scenarios which are located at the extremes of the network polygon. This way, while keeping our network subproblem tractable, we ensure that the network constraints are satisfied even for the worst combination of scenarios.

representative model, we use three types of consumers: *PV-Bat* consumers who own both a 5 kW/10 kWh battery with the round trip efficiency $\sigma^2 = 85\%$, as well as 5 kW rooftop PV, *PV* consumers who just own 5 kW rooftop PV, and *No-DER* consumers who are not equipped with any DER. We use anonymised solar and demand data of 27 consumers in Tasmania, Australia from [23], and randomly assign them to our 1410 consumers.

Our 1410 consumers are split equally between each of the consumer types (PV-Bat, PV, No-DER), and each of the consumers are being served by one of three aggregators. Aggregator 1 serves 250 PV-Bat and 270 PV consumers; aggregator 2 supplies 120 PV-Bat, 150 PV and 200 No-DER consumers; and aggregator 3 has 100 PV-Bat, 50 PV and 270 No-DER consumers. The aggregators' customers are at random nodes and multiple aggregators can have customers at the same node. Consumers in our system are consuming a total of 29 MWh per day on average, where aggregator 1, 2 and 3 are in charge of 10.5 MWh, 9 MWh, and 8.5 MWh, respectively. We solve our aggregator and network subproblems respectively using Gurobi and IPOPT solvers in JuMP, Julia [24] on a laptop computer with a 2.50 GHz Intel$^{(R)}$ Core$^{(TM)}$ i7 and 8 GB of memory.

B. NEMDE Implementation

More than 200 agents participate in the NEM energy and FCAS markets every day. NEMDE co-optimizes all these participants every five minutes, to obtain the market prices as well as the dispatch of every participants. Here, we implement a simplified version of NEMDE to dispatch our aggregators. To simplify, we assume that all the participants in the same market region (Australian states) are located at one transmission node. This leads to a transmission network with 5 nodes, each representing one of the Australian eastern states/territories. We assume our 141-bus distribution network is connected to the bus representing New South Wales (NSW). For each region, we extract the energy and FCAS bids of all participants as well as its demand and FCAS requirements from AEMO's website.[5] Similarly to NEMDE, we use a linear OPF to obtain the dispatch of all our participants (including our aggregators) and the price of each market.

C. Comparative Approaches

To illustrate the performance of our price-elastic approach, we compare the results of three different approaches:

Inelastic: in which aggregators optimize their portfolio using the optimization model (2a)–(2c). The optimization uses price forecasts provided by the AEMO's pre-dispatch. Both the predispatch and market clearing prices are provided in Fig. 5. The mean absolute error of the forecasts and the realized prices for energy, raise and lower FCAS market is 9.6, 7.4 and 3.0, respectively The demand bids are submitted at the cap price, and supply and FCAS bids are submitted at the floor price.

Perfect: in which aggregators optimize their portfolio using the optimization model (2a)–(2c). The optimization uses market clearing prices instead of forecasts for the whole horizon (288 future time steps). Similarly to Inelastic, the demand bids are submitted at the cap price, and supply and FCAS bids are submitted at floor prices.

[5]http://nemweb.com.au/

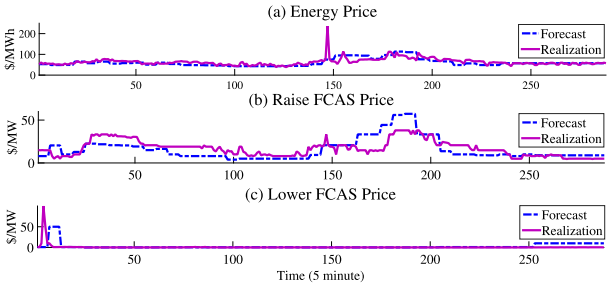

Fig. 5. Energy, Raise and Lower FCAS Market Prices.

TABLE II
OVERALL BENEFIT OF AGGREGATORS NEGLECTING NETWORK

Approach	Market	Total Benefit (AUD)				Rel. to InE (%)
		Agg. 1	Agg. 2	Agg. 3	Total	
Inelastic	Energy	124	-157	-266	742	–
	FCAS	554	266	222		
Perfect	Energy	242	-101	-219	991	33%
	FCAS	569	273	227		
Price-Elastic	Energy	214	-113	-230	896	21%
	FCAS	546	262	218		

Price-Elastic: in which aggregators run the proposed approach to generate their energy-FCAS regions (both raise and lower FCAS markets) as well as their price bands. Note that we use the same forecasts as in Inelastic to obtain the prices. Here, we only obtain three price bands each reflecting the price of a highly likely transition that aggregators can experience: 1) moving from the base case in which the batteries are neither charging nor discharging to charge mode; 2) moving from the base case to discharge mode; 3) moving from the base case in which all PV is curtailed to a no-PV-curtailed point. Note that we have tried 10 price-bands yet the additional aggregator benefits were negligible. The reason is that the aggregators problem is linear and these transitions, especially over a 5 minute settlement, are representative.

Note all the above approaches are implemented within a rolling horizon framework which moves forward one time step (5 minutes) at a time.

To highlight the effectiveness of bidding a wider range of DER operating points, we first report aggregators' benefit for the above approaches when the network constraints are neglected. Table II reports the one-day benefit of aggregators 1–3 (shown by Agg. 1 – Agg. 3) when participating in both energy and FCAS markets while neglecting the distribution network.

As reported in Table II, the proposed price-elastic approach could bring 21% higher benefits for aggregators compared to an inelastic approach. The reason is that inelastic approaches submit their bids at either floor or market cap prices, therefore, no matter how much the real price deviates from the forecasts, their bids are accepted by the market. However, our proposed approach bids different capacities for different prices, So, in case the real price deviates from the forecast, our approach can act differently to ensure that the highest

TABLE III
NETWORK AND REACTIVE POWER SUPPORT EFFECT

Approach	Total benefit (AUD)			Rel. to no Net. (%)
	First Net.	Fully Net.	Reactive	
Inelastic	732	734	742	(-1.3, -1.1, 0.0)
Perfect	969	979	991	(-2.2, -1.2, 0.0)
Price-Elastic	839	844	889	(-6.4, -5.8, -0.7)

benefit is achieved. Moreover, as can be seen in Table II, the perfect approach brings the highest benefit since it uses the market clearing prices (i.e., perfect information). Yet since the network constraints are neglected, the results in Table II might be infeasible.

Note that here, we allow prices to be updated in real-time, thus every iteration of our rolling horizon framework reflects the latest expected cost of aggregators. Yet, according to the current NEM regulations, the prices for the whole day needs to be submitted prior to the market day. To have an idea of how this requirement can change aggregators benefits, we clustered the price forecasts into 10 price bands using k-means [25] and used the centroids of these 10 clusters as the fixed prices. Then, in real time (when we obtain our prices), we select the closest match from these fixed prices instead of updating price bands. Since under these fixed prices aggregators do not have to reflect their true expected costs, in our experiments, they could obtain 7% higher benefits, compared to a case when they reflect their true costs. This means that a more sophisticated approach for determining prices could improve aggregators' benefit. However, we leave the detailed study of such a case to future work.

D. Inclusion of Network and Reactive Power Support

Here, we illustrate the effect of including the network and the reactive power support. To show the effectiveness of our network sub-problem, we report the results for two cases of network observability; First Net: where only the first time step of every rolling horizon iteration incorporates network constraints, i.e., remove constraint (5c) in the aggregator sub-problem and solve OPFs only for the first time step in the network sub-problem; and Fully Net: where every iteration solves multi-period OPFs over all the remaining time steps within a horizon. To provide a fair comparison, we include the network subproblems for both inelastic and perfect approaches. To do so, we use a similar approach as in Section V, yet instead of solving the network subproblem for the extreme points of aggregators energy-reserve region, we solve OPF for the operating point obtained by inelastic and perfect approaches.

Table III reports the total one-day benefits of our aggregators for the two network cases as well as a case when aggregators also provide reactive power support (Reactive) while using a Fully Net network model. For the Inelastic and Perfect cases we again use a similar approach as in Section IV-E to enable them to provide reactive power support.

The relative benefit improvement of the two network cases and the Reactive case w.r.t. no network case (i.e., Table II) is also reported in Table III. The first, second and third values are

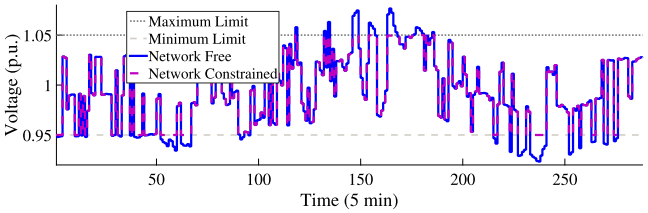

Fig. 6. The voltage of bus 141 in energy case.

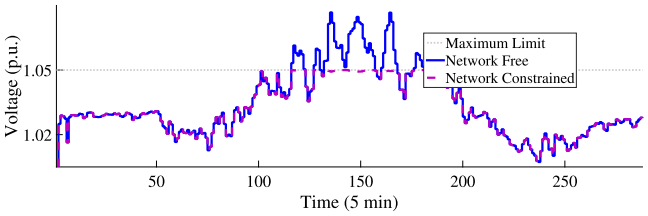

Fig. 7. The voltage of bus 141 in raise FCAS case.

respectively the relative benefit improvement of the First Net., Fully Net., and the Reactive case. Note that since the network constraints are included, all three cases obtain network feasible results; however, the highest benefit is obtained when aggregators also provide reactive power support. The reason is that such a support expands the network feasible region thus aggregators can bid with less restrictions.

E. Distribution Network Voltage Analysis

After market clearing when the real dispatch of each aggregator is revealed, we solve three PFs (one where no FCAS action is required (energy alone), one for max raise FCAS activation, and another where max lower FCAS is activated) to obtain the actual voltages at each node. We plot the voltage of node 141, in the normal operating condition and when the raise FCAS is deployed in Figures 6–7, respectively. Each figure plots two cases; one where the network was neglected when bidding (Network Free); another where the network was fully incorporated (Network Constrained).

As can be seen in Figs. 6 and 7, the voltage of node 141 is always within the safe limits for the proposed network-secure approach. Also, while the proposed approach could keep the voltage of all 141 nodes within the safe limits, 19 out of 141 nodes experienced at least one voltage violation in the Network Free case.

To show the impact of different curtailment policies when computing our network secure bids, we compare the bid curtailment under the L1 and L2 norms in the objective function (8a). Fig. 8 compares the amount of curtailed bids for the three highest prices[6] at time step 164, where the highest voltage violation occurs. As shown in the figure, unlike the L1 norm, the L2 norm mainly limits the most expensive bid. In our experiment, the L2 norm reduced the total aggregator benefit by 1.7% ($844 compared to $858). The reason is that when using an L1 norm, more expensive offers reach the market (leading to higher benefit for aggregators but at the expense of higher total operation cost from the market viewpoint). On

[6]There was no curtailment for prices lower than $77.

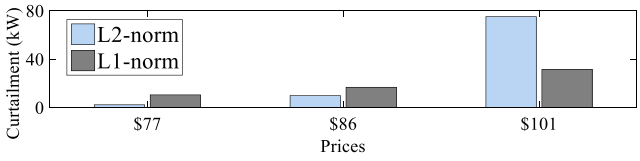

Fig. 8. Bid curtailment at different prices.

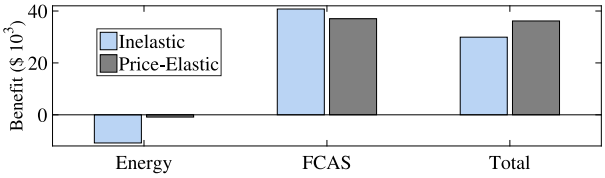

Fig. 9. Longer term Energy-FCAS benefit breakdown.

the other hand, our L2 norm curtailment policy ensures that the less expensive bids will make it to the market (leading to a lower total operation cost from the market viewpoint at the expense of a slightly less aggregator benefit).

F. Longer Term Cost Comparisons: Inelastic vs Proposed

Fig. 9 reports the total benefits of aggregator 1 together with the energy and FCAS shares when the aggregator uses the inelastic and our proposed price-elastic approach. This experiment is done over months September, October and November 2019, Australia. For both approaches, we have used AEMO's predispatch price forecast and then used our NEMDE to clear the market and obtain the real benefit of aggregators according to their dispatch. Our proposed approach delivered a 19% higher benefit over three months compared to the inelastic approach.

G. Computational Performance

Table IV reports the total problem size and the computational time of inelastic, perfect and price-elastic approaches for our sequential implementation together with the expected parallel time (using the time of the slowest subproblems at each iteration). Note that in the aggregator subproblem, the number of variables is linear in the number of consumers. The reason is that no two aggregators nor any two consumers of the same aggregators have common variables and constraints. Thus, the aggregator subproblem can be decomposed at the connection point of every consumer within a single rolling horizon iteration and each of the consumer subproblem can be solved in parallel. Each consumer subproblem being solved (for the price-elastic approach) includes 21k and 16k variables and constraints, respectively. Similarly, our network subproblem can be separated into one OPF for each time step[7] and each power flow case under consideration: energy, FCAS raise, FCAS lower. This reduces the number variables and constraints relevant to the parallel resolution of the network subproblem to 2k and 1.7k, respectively.

As can be seen in Table IV, the estimated parallel time to solve the inelastic and the proposed price-elastic approaches,

[7]Since there is no time coupling constraints in the network subproblem.

TABLE IV
PROBLEM SIZE AND COMPUTATION TIME

Approach	Problem-part	Problem Size #Var.	Problem Size #Cons.	Time(s) Seq(Parallel)
Inelastic / Perfect	Aggregator	18,680k	14,772k	272 (0.43)
	Network	2,701k	2,243k	281 (0.41)
	Total	23,347k	17,015k	553 (0.84)
Price-Elastic	Aggregator	30,919k	22,774k	378 (0.91)
	Network	3,247k	2,514k	387 (0.39)
	Total	34,166k	25,288k	765 (1.30)

TABLE V
CENTRAL V.S. ADMM OPF

Approach	Problem-part	Problem Size #Var.	Problem Size #Cons.	Time(s) Seq(Parallel)
Inelastic Central [10]	Aggregator + Network	10,232k	5,359k	–
Inelastic ADMM [12]	Aggregator	8,528k	6,091k	5250 (1.2)
	Network	1,705k	486k	3424 (1.5)
	Total	10,233k	6,577k	8674 (2.7)

for a single horizon, are respectively 0.84s and 1.30s. Note that these are potential solve times for a fully parallel implementation. However, if the computational resources are not available to perform a fully parallel solve, and the solve time becomes a limiting factor, it is possible to approximate the problem by using a variable time discretisation of the horizon to reduce the number of time steps [23]. By using 30-minute steps after the first time step in the horizon, experiments show that we are able to reduce the sequential solve time 16 fold, at the cost of a 6% decrease in overall benefits.

H. DSO-Aggregator Setting

We initially designed our approach for the case where multiple independent aggregators share the same grid. However, we believe that our approach is also useful in the case where the same party acts both as a DSO and the sole aggregator. The reason is that modeling the constraints and variables of numerous consumers together with the grid OPFs leads to a large-scale multi-period problem which the DSO-aggregator might not be able to solve centrally (especially for realistically-sized distribution networks). To show this, we have studied a similar approach as in [10] in which a DSO uses a central OPF to obtain network-secure inelastic bids for the wholesale market. As reported in Table V, we could not solve this problem via state-of-the-art solvers on a laptop computer with 8 GB of memory (shown by "–" in Table V). The alternating direction method of multiplier (ADMM) is used in the literature to solve OPF in a distributed manner, which yields an approach capable of leveraging parallel computation similar to [12], and whose run-time is also reported in Table V. However, the ADMM approach in [12] is still an inelastic method which cannot offer a wide range of DER flexibility. Since the parallel run-time and objective function of our elastic approach in this DSO-aggregator setting is the same as that in the DSO + multiple aggregators setting, the results in Tables III and IV show that our elastic approach brings 15% higher benefits in total compared to the ADMM work in [12]

($844 compared to $737) whilst remaining computationally feasible.

VII. Conclusion

In this article, we answer the important question of how aggregators, who share the same distribution network, can efficiently participate in the energy and reserve markets while respecting the grid constraints. Unlike the common inelastic approaches, our approach generates bids and the prices for aggregators' whole flexibility. By obtaining the grid operating region, we also ensure that aggregators bids will not go beyond the network capabilities.

We illustrated the effectiveness of our approach using three aggregators who in total serve 1410 consumers in a 141-bus network. Our results show 19% improvement on aggregators benefit compared to an inelastic method. We also show the importance of network inclusion by using two network scenarios: A) the inclusion of the network just for the first time step, 2) the inclusion of the network for all the future time steps. While the network was feasible for both cases, the aggregator could obtain 0.6% higher benefits when they received the network visibility for the next 24 hours. We also show that if aggregators provide the network with their reactive power support, they can obtain about 5% higher benefits since such a reactive power support can expand the network feasible region.

In this article we primarily focus on the security of the network while opening up network capacity. However, our network subproblem can be extended to additionally consider reducing losses. Including different DER types and uncertainty (other than what our rolling horizon can capture) are two other possible extensions that we leave to future work.

References

[1] Y. Ding *et al.*, "Ecogrid EU-A large scale smart grids demonstration of real time market-based integration of numerous small DER and DR," in *Proc. 3rd IEEE PES Innovat. Smart Grid Technol. Europe (ISGT Europe)*, 2012, pp. 1–7.

[2] M. G. Vayá and G. Andersson, "Optimal bidding strategy of a plug-in electric vehicle aggregator in day-ahead electricity markets under uncertainty," *IEEE Trans. Power Syst.*, vol. 30, no. 5, pp. 2375–2385, Sep. 2015.

[3] Y. Wang, H. Liang, and V. Dinavahi, "Two-stage stochastic demand response in smart grid considering random appliance usage patterns," *IET Gener. Transm. Distrib.*, vol. 12, no. 18, pp. 4163–4171, 2018.

[4] J. P. Iria, F. J. Soares, and M. A. Matos, "Trading small prosumers flexibility in the energy and tertiary reserve markets," *IEEE Trans. Smart Grid*, vol. 10, no. 3, pp. 2371–2382, May 2019.

[5] S.-J. Lee *et al.*, "Coordinated control algorithm for distributed battery energy storage systems for mitigating voltage and frequency deviations," *IEEE Trans. Smart Grid*, vol. 7, no. 3, pp. 1713–1722, May 2016.

[6] S. Ø. Ottesen, A. Tomasgard, and S.-E. Fleten, "Multi market bidding strategies for demand side flexibility aggregators in electricity markets," *Energy*, vol. 149, pp. 120–134, Apr. 2018.

[7] E. Yao, V. W. S. Wong, and R. Schober, "Optimization of aggregate capacity of PEVs for frequency regulation service in day-ahead market," *IEEE Trans. Smart Grid*, vol. 9, no. 4, pp. 3519–3529, Jul. 2018.

[8] D. Zhu and Y.-J. A. Zhang, "Optimal coordinated control of multiple battery energy storage systems for primary frequency regulation," *IEEE Trans. Power Syst.*, vol. 34, no. 1, pp. 555–565, Jan. 2019.

[9] N. Neyestani, M. Y. Damavandi, M. Shafie-Khah, A. G. Bakirtzis, and J. P. S. Catalão, "Plug-in electric vehicles parking lot equilibria with energy and reserve markets," *IEEE Trans. Power Syst.*, vol. 32, no. 3, pp. 2001–2016, May 2017.

[10] B. Vatandoust, A. Ahmadian, M. A. Golka, A. Elkamel, A. Almansoori, and M. Ghaljehei, "Risk-averse optimal bidding of electric vehicles and energy storage aggregator in day-ahead frequency regulation market," *IEEE Trans. Power Syst.*, vol. 34, no. 3, pp. 2036–2047, May 2019.

[11] N. Good and P. Mancarella, "Flexibility in multi-energy communities with electrical and thermal storage: A stochastic, robust approach for multi-service demand response," *IEEE Trans. Smart Grid*, vol. 10, no. 1, pp. 503–513, Jan. 2019.

[12] A. Attarha, P. Scott, and S. Thiébaux, "Network-aware co-optimisation of residential DER in energy and FCAS markets," *Electr. Power Syst. Res.*, vol. 189, Dec. 2020, Art. no. 106730.

[13] A. Attarha, P. Scott, and S. Thiébaux, "Network-aware participation of aggregators in NEM energy and FCAS markets," in *Proc. 11th ACM Int. Conf. Future Energy Syst.*, 2020, pp. 14–24.

[14] B. Cheng and W. B. Powell, "Co-optimizing battery storage for the frequency regulation and energy arbitrage using multi-scale dynamic programming," *IEEE Trans. Smart Grid*, vol. 9, no. 3, pp. 1997–2005, May 2018.

[15] S. Shafiee, H. Zareipour, and A. M. Knight, "Developing bidding and offering curves of a price-maker energy storage facility based on robust optimization," *IEEE Trans. Smart Grid*, vol. 10, no. 1, pp. 650–660, Jan. 2019.

[16] J. Arteaga and H. Zareipour, "A price-maker/price-taker model for the operation of battery storage systems in electricity markets," *IEEE Trans. Smart Grid*, vol. 10, no. 6, pp. 6912–6920, Nov. 2019.

[17] Z. Zhou, T. Levin, and G. Conzelmann, "Survey of U.S. ancillary services markets," Argonne Nat. Lab., Lemont, IL, USA, Rep. ANL/ESD-16/1, 2016.

[18] J. Riesz, J. Gilmore, and I. MacGill, "Frequency control ancillary service market design: Insights from the Australian National Electricity Market," *Electricity J.*, vol. 28, no. 3, pp. 86–99, Apr. 2015.

[19] B. Xu, J. Zhao, T. Zheng, E. Litvinov, and D. S. Kirschen, "Factoring the cycle aging cost of batteries participating in electricity markets," *IEEE Trans. Power Syst.*, vol. 33, no. 2, pp. 2248–2259, Mar. 2018.

[20] A. E. M. Operator, *Guide to Ancillary Services in the National Electricity Market*, Aust. Energy Market Operat., Melbourne, Australia, 2015.

[21] M. Farivar and S. H. Low, "Branch flow model: Relaxations and convexification—Part I," *IEEE Trans. Power Syst.*, vol. 28, no. 3, pp. 2554–2564, Aug. 2013.

[22] M. Z. Liu *et al.*, "On the fairness of PV curtailment schemes in residential distribution networks," *IEEE Trans. Smart Grid*, vol. 11, no. 5, pp. 4502–4512, Sep. 2020.

[23] P. Scott, D. Gordon, E. Franklin, L. Jones, and S. Thiébaux, "Network-aware coordination of residential distributed energy resources," *IEEE Trans. Smart Grid*, vol. 10, no. 6, pp. 6528–6537, Nov. 2019.

[24] I. Dunning, J. Huchette, and M. Lubin, "Jump: A modeling language for mathematical optimization," *SIAM Rev.*, vol. 59, no. 2, pp. 295–320, 2017.

[25] M. Ramezani, C. Singh, and M.-R. Haghifam, "Role of clustering in the probabilistic evaluation of TTC in power systems including wind power generation," *IEEE Trans. Power Syst.*, vol. 24, no. 2, pp. 849–858, May 2009.